

## **Structural Basis for the Mutation-Induced Dysfunction of Human IL-15 in Complex with IL-15 $\alpha$ Receptor**

**Zahida Batool<sup>a</sup>, Urooj Qureshi<sup>a</sup>, Mamona Mushtaq<sup>b</sup>, Sarfaraz Ahmed<sup>c</sup>, Mohammad Nure-Alam<sup>c</sup>, Zaheer Ul-Haq<sup>a,b\*</sup>**

<sup>a</sup>H.E.J Research Institute of Chemistry, International Center for Chemical and Biological Sciences, University of Karachi-75270, Karachi, Pakistan.

<sup>b</sup>Dr. Panjwani Center for Molecular Medicine and Drug Research, International Center for Chemical and Biological Sciences, University of Karachi-75270, Karachi, Pakistan.

<sup>c</sup>*Department of Pharmacognosy, College of Pharmacy, King Saud University, P.O. Box. 2457, Riyadh 11451, Kingdom of Saudi Arabia*

Table S1. Calculated binding free energy and the individual energy terms (kcal/mol) of hot spot residues of WT and mutated systems, calculated using HawkDock webserver.

<b>System</b>	<b>Residue</b>	$\Delta E_{vdw}$	$\Delta E_{ELE}$	$\Delta G_{GB}$	$\Delta G_{SA}$	$\Delta G_{MMGBSA}$
<b>WT</b>	Pro-Recp	-53.22	-1454.33	1429.03	-8.41	-86.93
	26	-4.37	1.47	0.35	-0.53	-3.07
	46	-0.27	-110.08	100.74	-0.25	-9.86
	53	-3.37	-87.59	88.56	-0.71	-3.11
	89	-2.86	-113.26	111.56	-0.85	-5.41
<b>Y26N</b>	Pro-Recp	-44.68	-1314.71	1334.69	-6.20	-30.9
	26	-1.58	-4.41	3.92	-0.29	-2.36
	46	-1.65	-89.33	89.02	-0.24	-2.21
	53	-2.86	-79.39	81.86	-0.65	-1.03
	89	-1.95	-77.92	78.99	-0.48	-1.36
<b>E46R</b>	Pro-Recp	-79.6	-1185	1194.89	-11.16	-81.85
	26	-3.79	-0.75	0.57	-0.59	-4.57
	46	-0.26	48.21	-46.94	0.00	1.01
	53	-4.83	-101.99	103.25	-0.68	-4.25
	89	-2.24	-56.02	58.37	-0.58	-0.47
<b>E53R</b>	Pro-Recp	-64.83	-1113.13	1121.70	-8.72	-64.97
	26	-4.91	2.72	-0.22	-0.48	-2.89
	46	-0.83	-107.66	99.35	-0.29	-9.43
	53	-3.67	47.97	-44.2	-0.66	-0.57
	89	-4.82	-83.31	86.51	-0.77	-2.39
<b>E89R</b>	Pro-Recp	-64.67	-1175.10	1173.72	-9.79	-75.85
	26	-4.23	-2.71	1.72	-0.51	-5.73
	46	-0.23	-114.31	105.60	-0.30	-9.23
	53	-1.81	-54.31	54.27	-0.29	-2.14
	89	-3.54	51.47	-48.55	-0.62	-1.24

Table S2. The overview of the interchain hydrogen bonds in native and mutated systems.

Systems	IL-15	IL-15R $\alpha$	H- Bond Distances
WT	Y26	R35	2.82
	D22	R26	3.15
Y26N	-	-	-
E46R	E53	R24; S41; L42	3.48; 2.75; 2.87
	D22	K17	3.12
	T24	R35	3.45
E53R	E46	R35; G38; T39	3.11; 2.90; 3.19
	Y26	R35	2.59
	E89	A37	2.83
	<b>R53</b>	R24	3.06
E89R	E53	R24	3.36
	T26	R35	2.61
	R89	K34	3.23
	C88	K34	3.10
	E46	R35; G38	3.42; 2.76
	E87	L36	3.04
	T24	R35	2.97

Table S3. The overview of the interchain hydrophobic interactions in native and mutated systems.

Systems	IL-15	IL-15R $\alpha$	Distances
<b>WT</b>	Y26	R35; L34; L36; A37	4.12; 4.19; 4.44; 4.32
	E46	R35; A37; G38	4.04; 3.75; 3.93
	E53	R24; S40; S41; L42	4.16; 3.83; 3.80; 3.98
	E89	K34; R35; K36; A37; I64	3.99; 4.11; 3.95; 4.11; 3.80
<b>Y26N</b>	E46	A37; G38	4.08; 4.12
	E53	S41; L42; R26	4.09; 4.23; 4.01
	E89	I64	3.85
<b>E46R</b>	Y26	C29; K34; R35	4.39; 4.21; 4.10
	E53	R35; R24; T39; S40; S41; L42	4.25; 4.48; 3.97; 4.12; 3.66; 4.01
	E89	R35; A37; I64; P67	4.19; 4.26; 3.99; 4.34
<b>E53R</b>	Y26	K34; R35; K36; A37	4.01; 3.95; 4.17; 3.94
	E46	R35; K36; A37; G38; T39	4.07; 4.30; 3.90; 3.99; 4.10
	R53	R24; L44	4.92; 3.90
	E89	K34; R35; K36; A37; I64	3.94; 3.96; 4.13; 3.98; 4.14
<b>E89R</b>	Y26	K34; R35; K36; A37	4.09; 3.95; 4.24; 4.18
	E46	R35; A37; G38; T39	4.03; 3.91; 4.02; 4.45
	E53	R24; L42	4.19; 3.86
	R89	K34; I64; P67	4.28; 4.10; 3.93

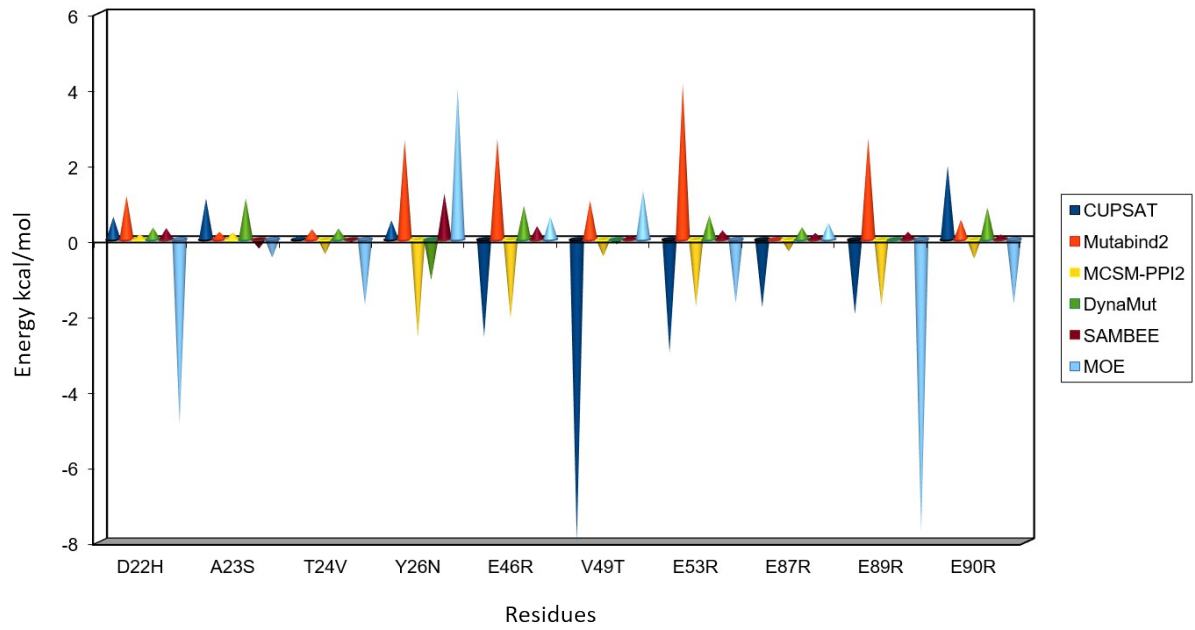


Figure S1. Comparison of binding free energies of pocket residues between mutational tools CUPSAT, Mutabind2, MCSM-PPI2, DynaMut, SAMBEE and MOE.

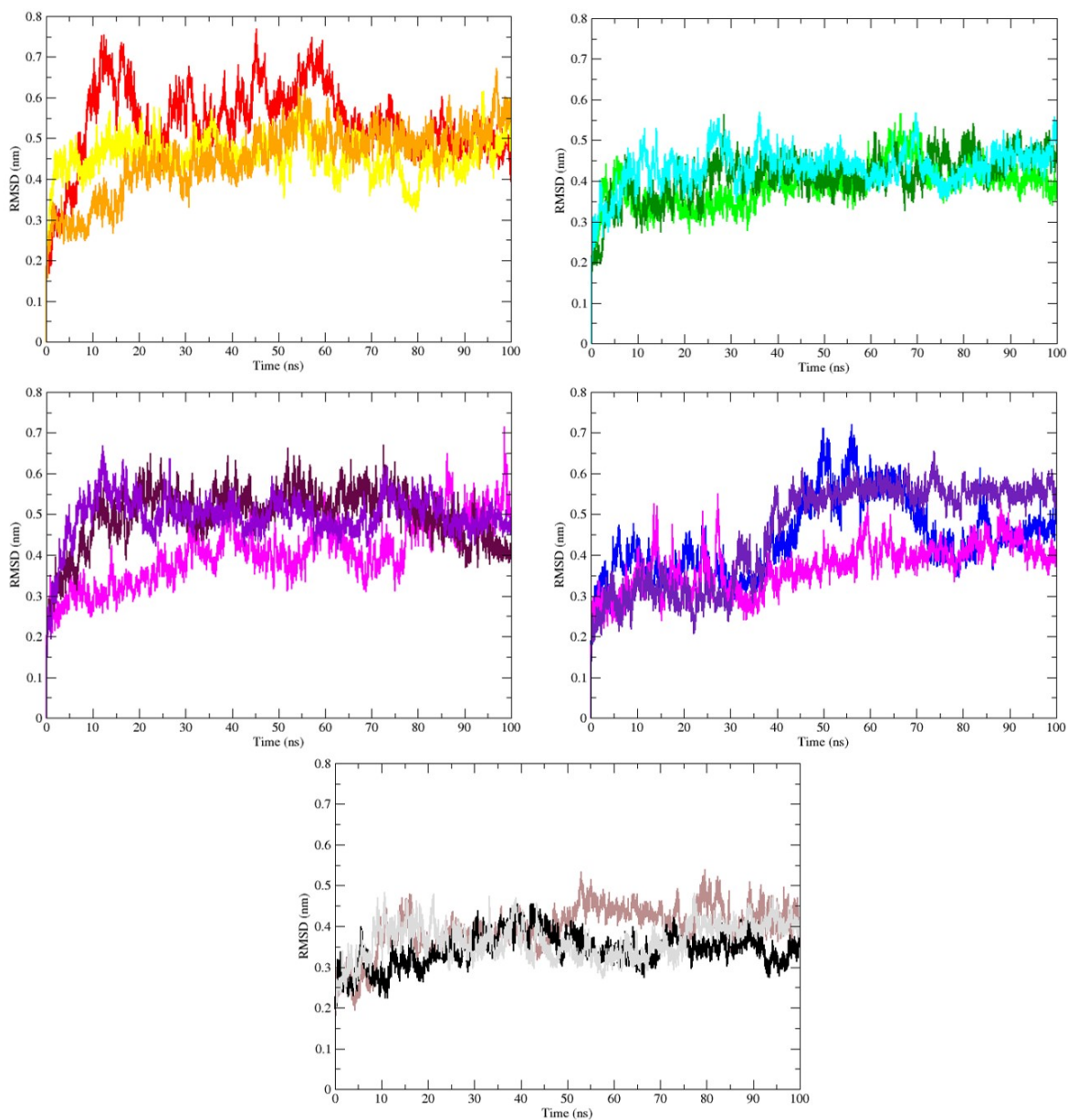


Figure S2. Root Mean Square Deviation (RMSD) of triplicates (t1-t3); Y26N t1 in red, t2 in orange and t3 in yellow color, E46R t1 in green, t2 in cyan and t3 in dark red color, E53R t1 in magenta color, t2 in violet and t3 in brown color, E89R t1 in blue, t2 in indigo and t3 in magenta color and WT t1 in black, t2 in brown and t3 in grey color

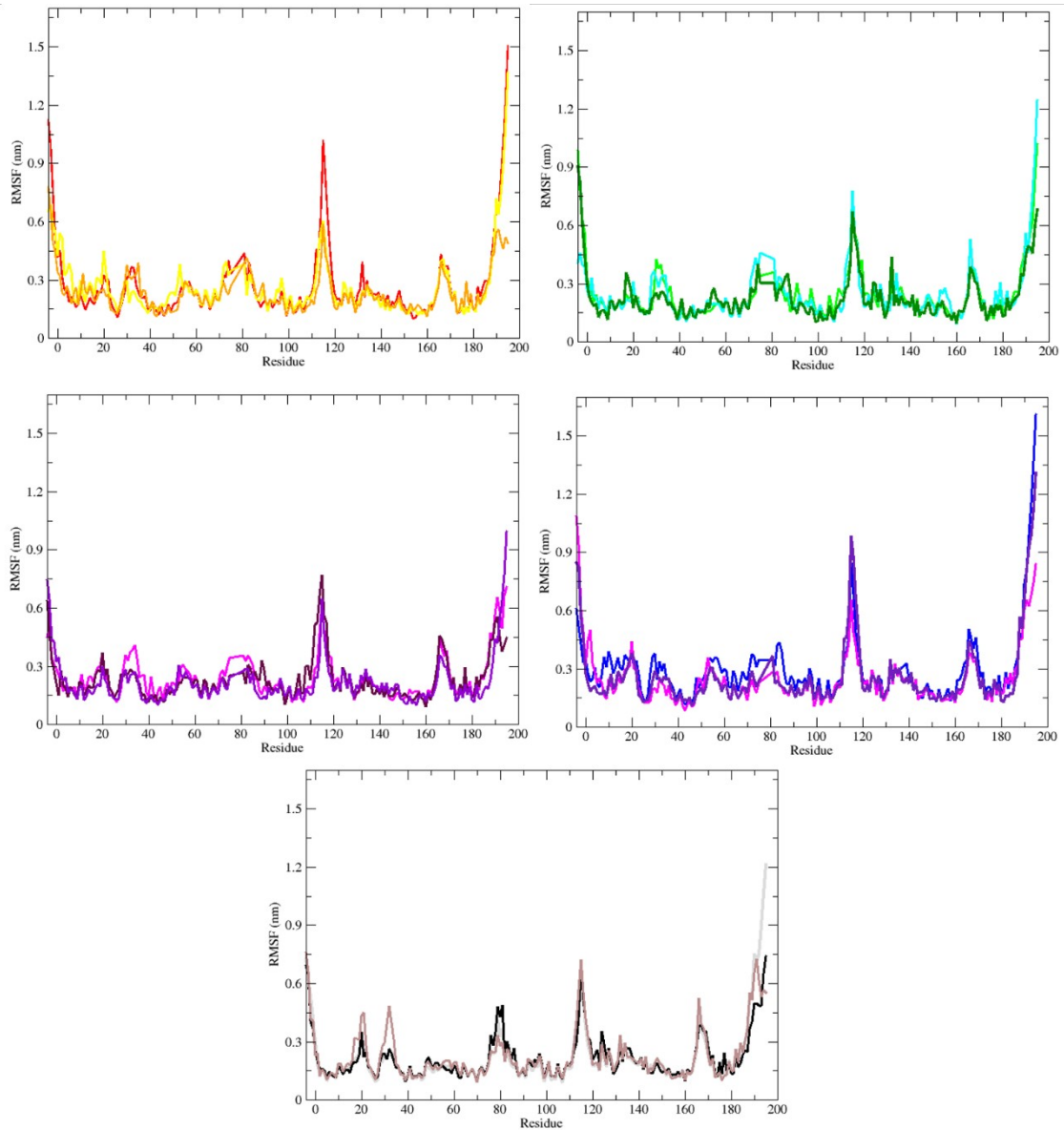


Figure S3. Root Mean Square Fluctuation (RMSF) of triplicate (t1-t3); Y26N; t1 in red, t2 in orange and t3 in yellow color, E46R; t1 in green, t2 in cyan and t3 in dark red color, E53R; t1 in magenta color, t2 in violet and t3 in brown color, E89R; t1 in blue, t2 in indigo and t3 in magenta color and WT; t1 in black, t2 in brown and t3 in grey color

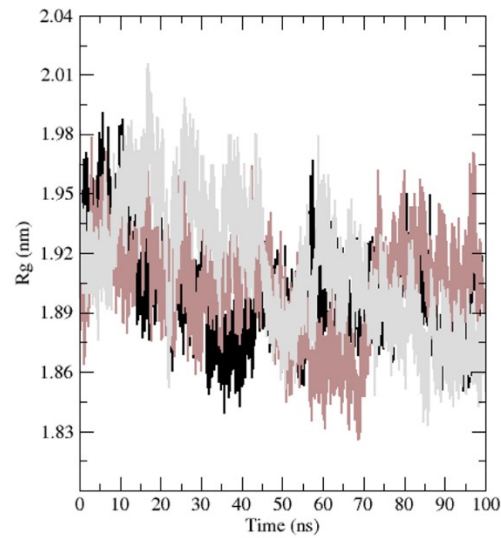
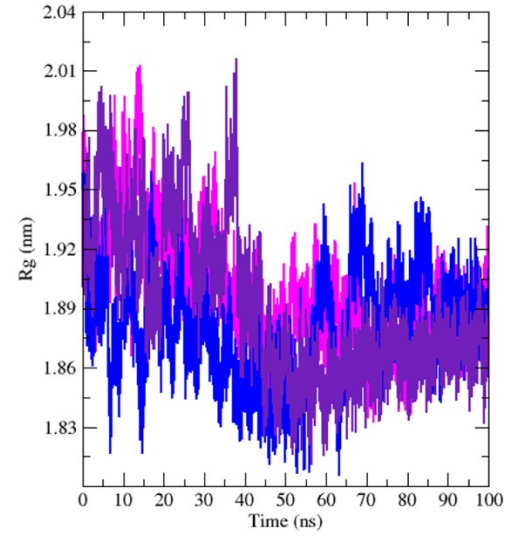
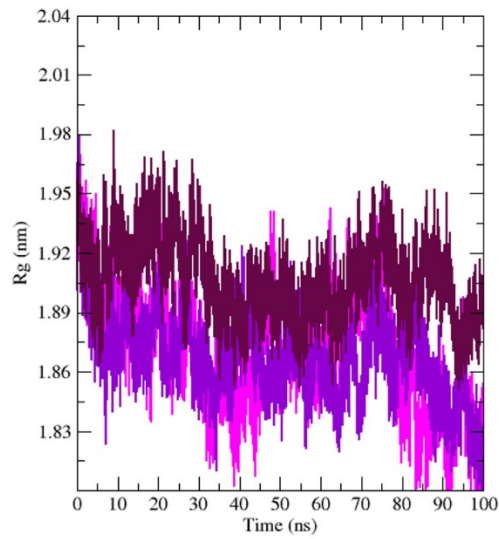
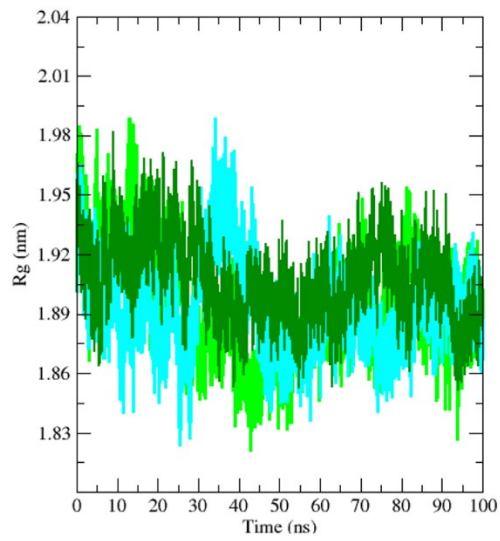
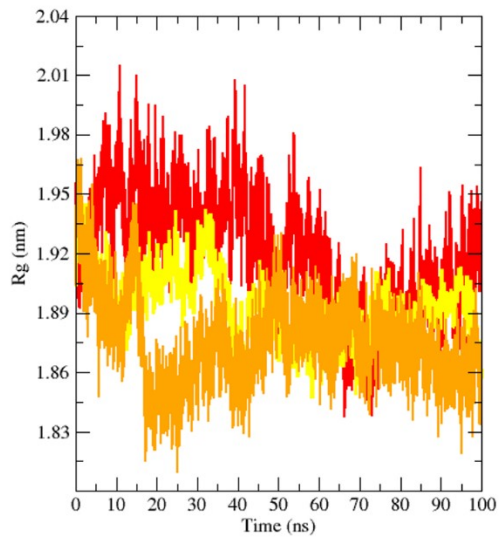




Figure S4. Radius of Gyration ( $R_g$ ) of triplicates (t1-t3); Y26N; t1 in red, t2 in orange and t3 in yellow color, E46R; t1 in green, t2 in cyan and t3 in dark red color, E53R; t1 in magenta color, t2 in violet and t3 in brown color, E89R; t1 in blue, t2 in indigo and t3 in magenta color and WT; t1 in black, t2 in brown and t3 in grey color.

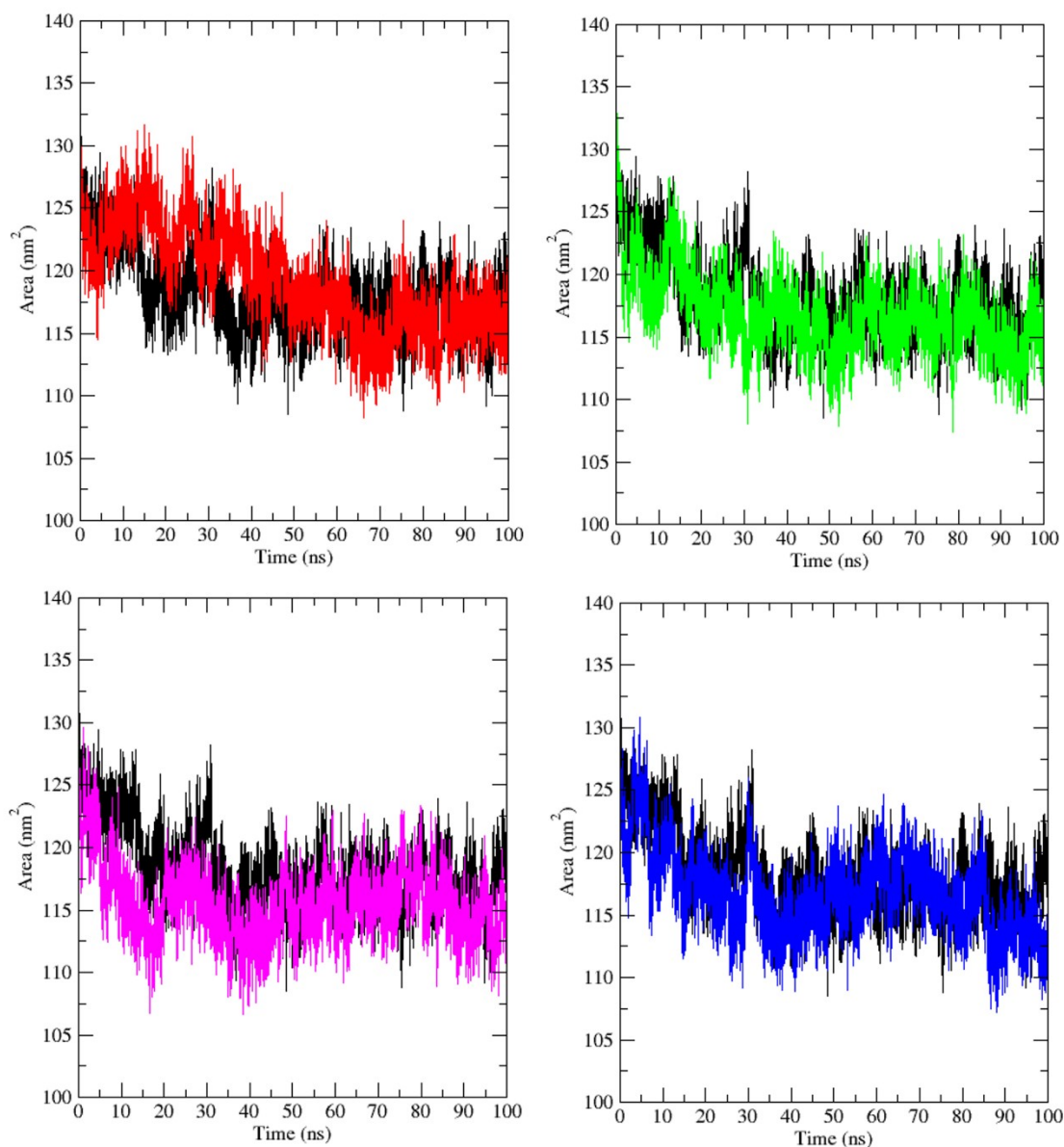


Figure S5. The Solvent Accessible Surface Area (SASA) plot of wild type (black), Y26N (red), E46R (green), E53R (magenta), and E89R (blue) over 100 ns of simulation.

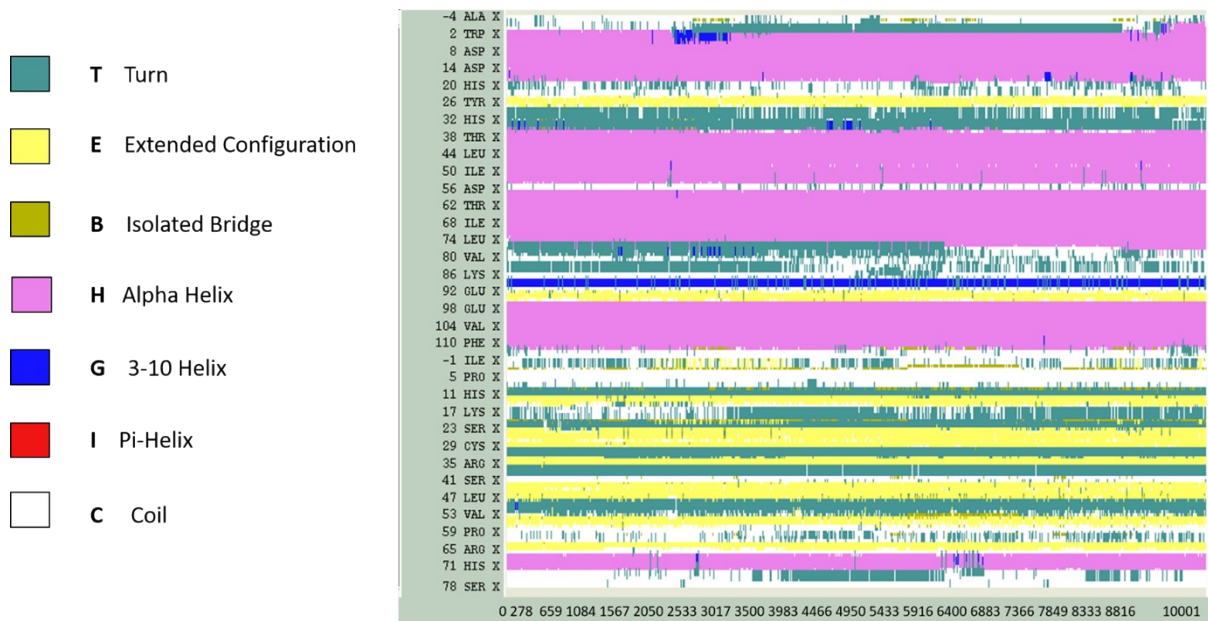


Figure S6. Secondary structure analysis of the wild type.

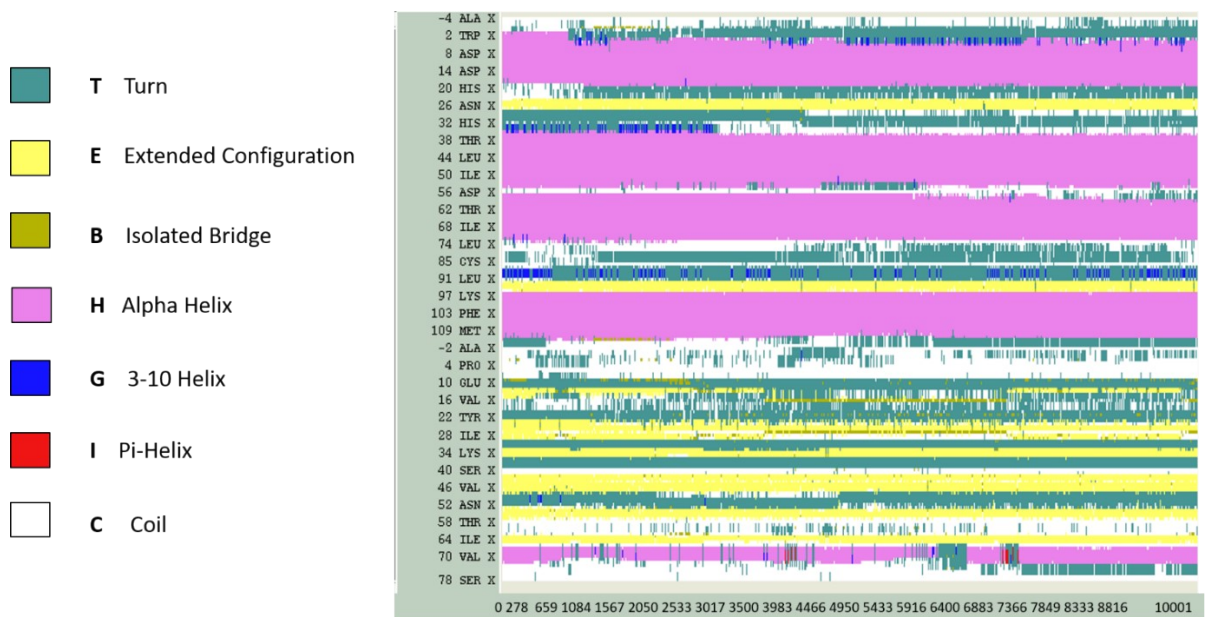


Figure S7. Secondary structure analysis of the Y26N mutant.

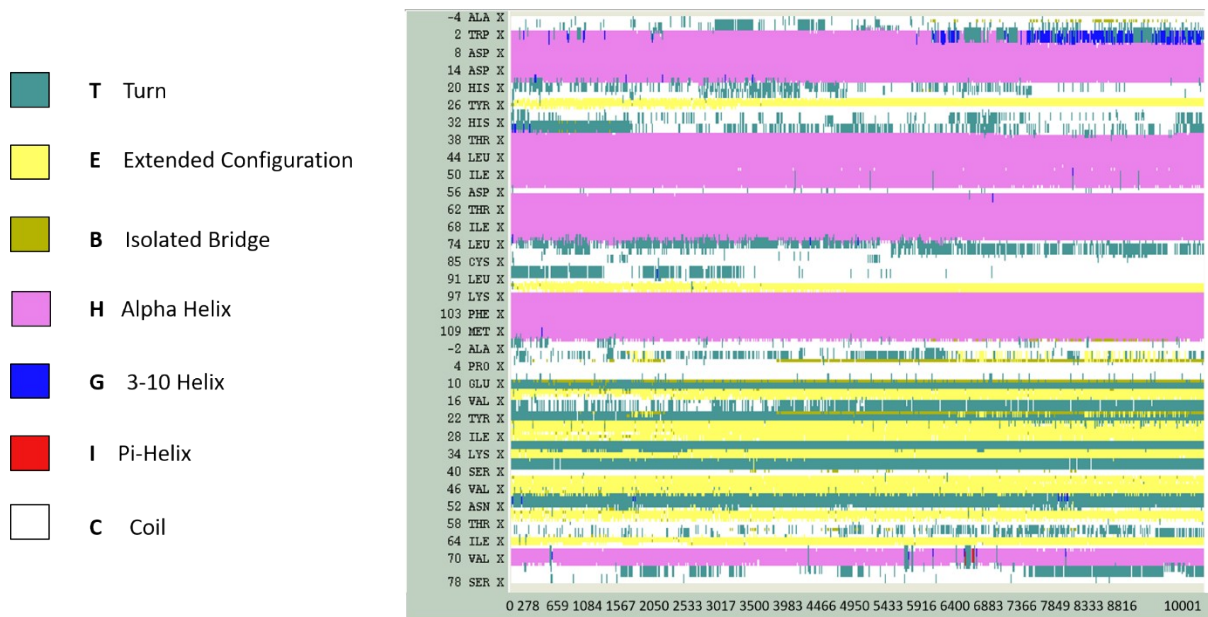


Figure S8. Secondary structure analysis of the E46R mutant.

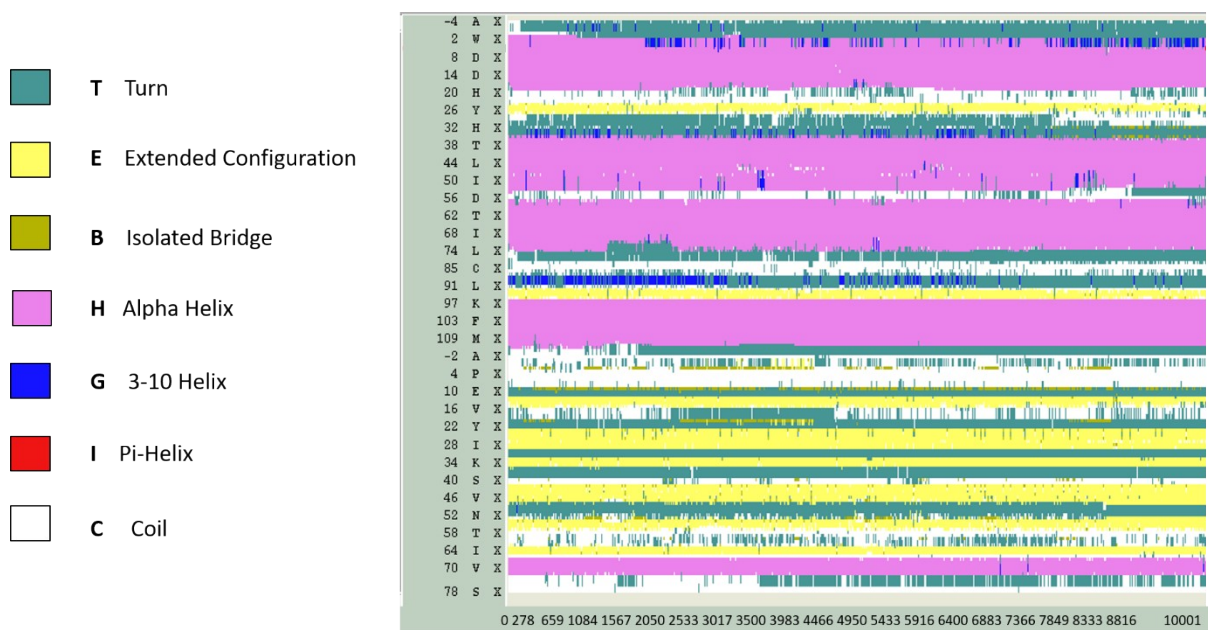


Figure S9. Secondary structure analysis of the E53R mutant.

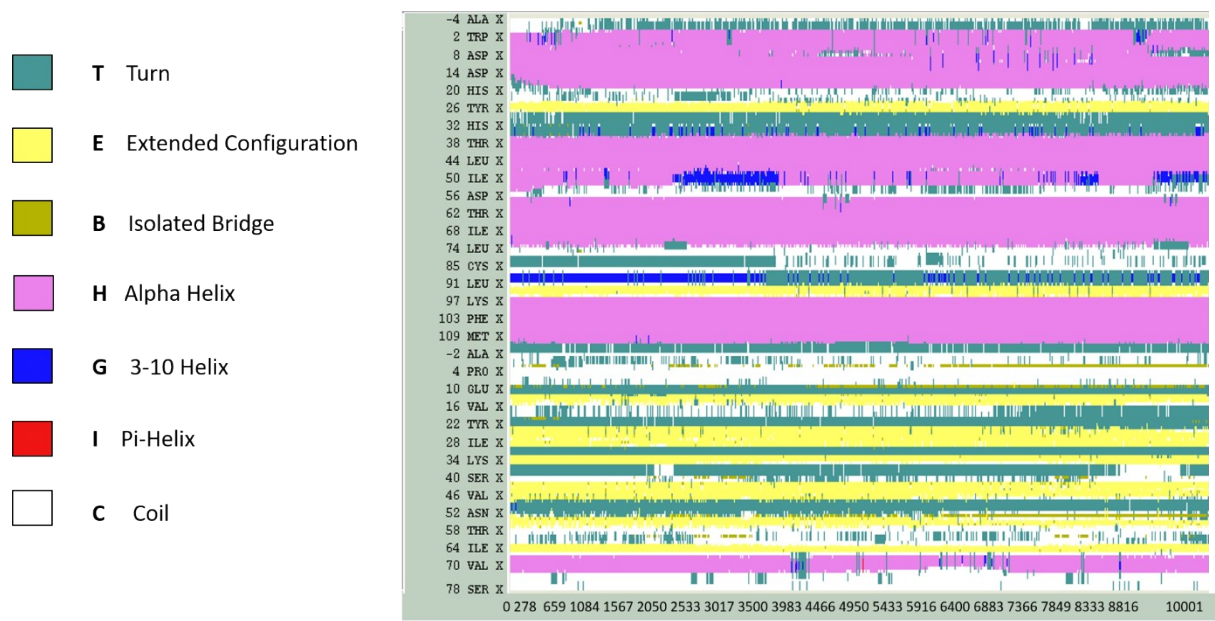


Figure S10. Secondary structure analysis of the E89R mutant.